Pergamon

TETRAHEDRON

Tetrahedron 57 (2001) 3537–3547

Reaction of cyclopropenylium ions with the *tert*-butyl-C_{60} anion: carbocation–carbanion coordination vs salt formation

Toshikazu Kitagawa,* Toru Tanaka, Hideyuki Murakita, Atsunori Nishikawa and Ken'ichi Takeuchi

Department of Energy and Hydrocarbon Chemistry, Graduate School of Engineering, Kyoto University, Sakyo-ku, Kyoto 606-8501, Japan

Received 15 September 2000; accepted 22 November 2000

Abstract—The reaction of the *tert*-butyl-C_{60} anion (t-BuC_{60}^-) with tricyclopropylcyclopropenylium ion and 1,2-dicyclopropyl-3-(4-methylphenyl)cyclopropenylium ion underwent C–C covalent bond formation to give 1-*tert*-butyl-4-(2-cyclopropen-1-yl)-1,4-dihydro[60]fullerenes. The newly formed C–C bond of these hydrocarbons was found to undergo reversible heterolysis in polar solvents to give the original ions. A more highly stabilized carbocation tris[1-(5-isopropyl-3,8-dimethylazulenyl)]cyclopropenylium ion did not react with t-BuC_{60}^-, and a hydrocarbon with a salt structure was isolated as a solid. Tri-*tert*-butylcyclopropenylium ion, although less stable than the other cations, underwent no C–C bond formation with t-BuC_{60}^-, indicating that steric hindrance effectively suppresses carbocation–carbanion coordination. These results provide a demonstration of a change in reactivity between t-BuC_{60}^- and substituted cyclopropenylium ions toward C–C coordination, depending on the thermodynamic stability and steric crowding of the cation. © 2001 Elsevier Science Ltd. All rights reserved.

1. Introduction

A high electron affinity, induced by the spherical π-conjugated system, is a characteristic property of fullerene C_{60}. In addition to the widely studied reduction of C_{60} to give a radical anion,[1] the deprotonation of the highly acidic monosubstituted dihydrofullerenes $RC_{60}H$, to give a stable carbanion RC_{60}^-, is noteworthy. The parent molecule of this family, $C_{60}H_2$, which is known to have a 1,2-addition structure in its most stable form, has a pK_a of 4.7.[2] A variety of monosubstituted 1,2-dihydro[60]fullerenes are known, and the acidic character of these has been experimentally demonstrated by several groups.[3–6] Among these, the cyano and *tert*-butyl derivatives have been reported to have pK_as of 2.5[5] and 5.7,[6,7] respectively. The pK_a studies of 1,2-$C_{60}H_2$ and 1,2-t-$BuC_{60}H$ have shown that dihydrofullerenes constitute a family of the most acidic hydrocarbons known today. These hydrocarbons have also been the subject of theoretical studies by molecular orbital calculations, which have concluded that the highly acidic character of these compounds can be explained by the electron delocalization upon ionization.[9]

In earlier studies, we showed that the ionization of a hydrocarbon can occur at a C–C bond, if the resulting carbocation and carbanion are sufficiently stabilized.[10–12] Such hydrocarbons are unusual, because hydrocarbon ions are generally thought to be highly reactive species. Using a large hydrocarbon anion, stabilized by a planar π-conjugated system, we synthesized the first hydrocarbon to contain an ionically dissociable C–C bond and also showed that some of these hydrocarbons can be isolated as ionic solids, i.e. as hydrocarbon salts.[11,13] The known acidity of $RC_{60}H$ suggests that the conjugate base RC_{60}^- is also sufficiently stable to serve as an anionic moiety of ionically dissociable molecules. In fact, it was found that a series of hydrocarbons t-BuC_{60}-**1** undergo reversible and clean heterolysis into ions in polar media (Scheme 1).[14,15]

In this respect, the cyclopropenylium ion, another Hückel aromatic cation, would be a candidate for a cationic component of such unusual hydrocarbons. This paper describes the result of our studies of the reaction of t-BuC_{60}^- with cations $\mathbf{2}^+$,[16] $\mathbf{3}^+$,[11c,d] $\mathbf{4}^+$,[17] and $\mathbf{5}^+$,[18] with different stabilities and steric bulkiness.[19] The known pK_{R^+} values,[11c,16b,18b,19b] a carbocation thermodynamic stability parameter, are shown in Scheme 2.

2. Results and discussion

2.1. Reaction of t-BuC_{60}^- with 2^+ and 3^+

A dark green colored THF solution of t-BuC_{60}^- was prepared by deprotonation of *tert*-butyl-1,2-dihydro[60]fullerene (1,2-t-$BuC_{60}H$)[6,20] with t-BuOK. The addition of

---

Keywords: carbanions; carbenium ions; electrochemistry; fullerenes; hydrocarbons; ionization; solvents and solvent effects; substituent effects.

* Corresponding author. Tel.: +81-75-753-5713; fax: +81-75-753-3350; e-mail: kitagawa@scl.kyoto-u.ac.jp

PII: S0040-4020(01)00236-8

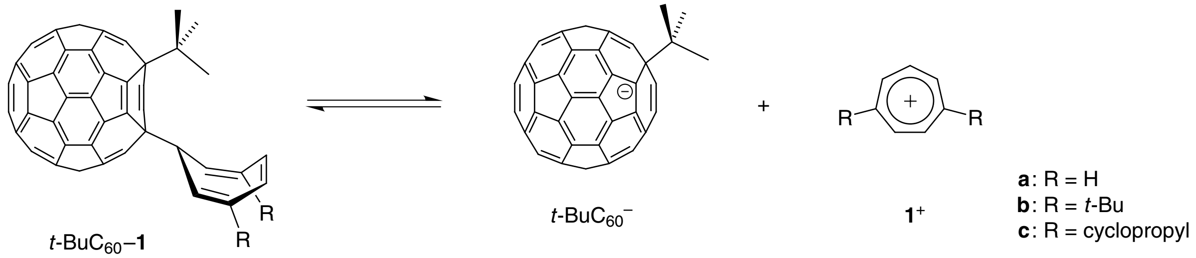

Scheme 1.

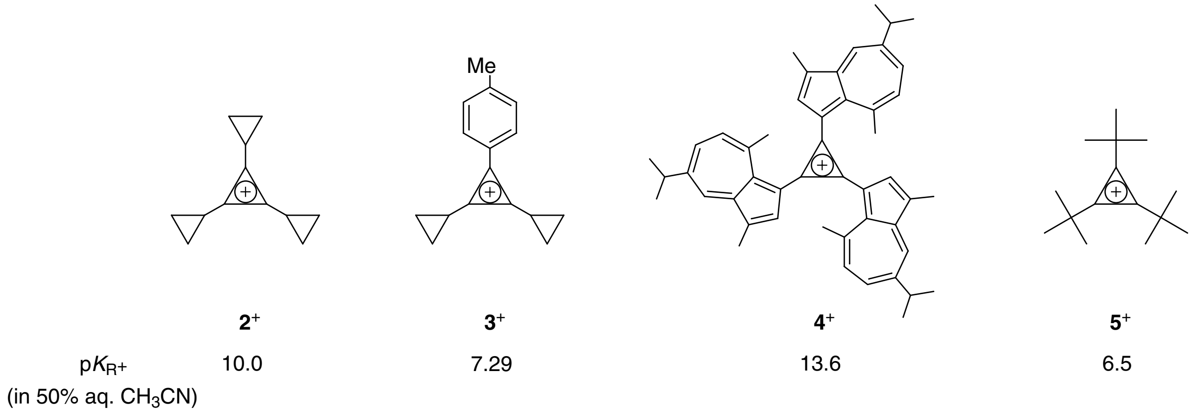

Scheme 2.

$2^+BF_4^-$or $3^+ClO_4^-$ resulted in the immediate disappearance of the green color, indicating the consumption of t-BuC_{60}^- by C–C covalent bond formation. The product was separated from the inorganic component (KBF_4 or $KClO_4$) by evaporation of the solvent and extraction with CS_2. Evaporation of the CS_2 yielded the coordination products (t-BuC_{60}-**2** and t-BuC_{60}-**3**) in quantitative yields as dark brown solids (Scheme 3).

NMR analysis indicated that t-BuC_{60}-**2** consists of only a single isomer. PM3 calculations of t-BuC_{60}^- have shown that the negative charge and HOMO coefficient are greatest at C-2 and second greatest at C-4.[15] The 1,2-isomer has C_s symmetry, whereas the 1,4-isomer has no symmetry (C_1). The NMR data are consistent with the formation of the 1,4-adduct, since all the protons and carbons, other than those of the *tert*-butyl group, exhibit unequal chemical shifts. It should be noted that one methine carbon is significantly more deshielded (δ 18.4) than the other two (δ 6.9 and 6.5). This signal is tentatively assigned to the cyclopropyl group attached to the sp^3 carbon of the cyclopropenyl ring (Fig. 1).

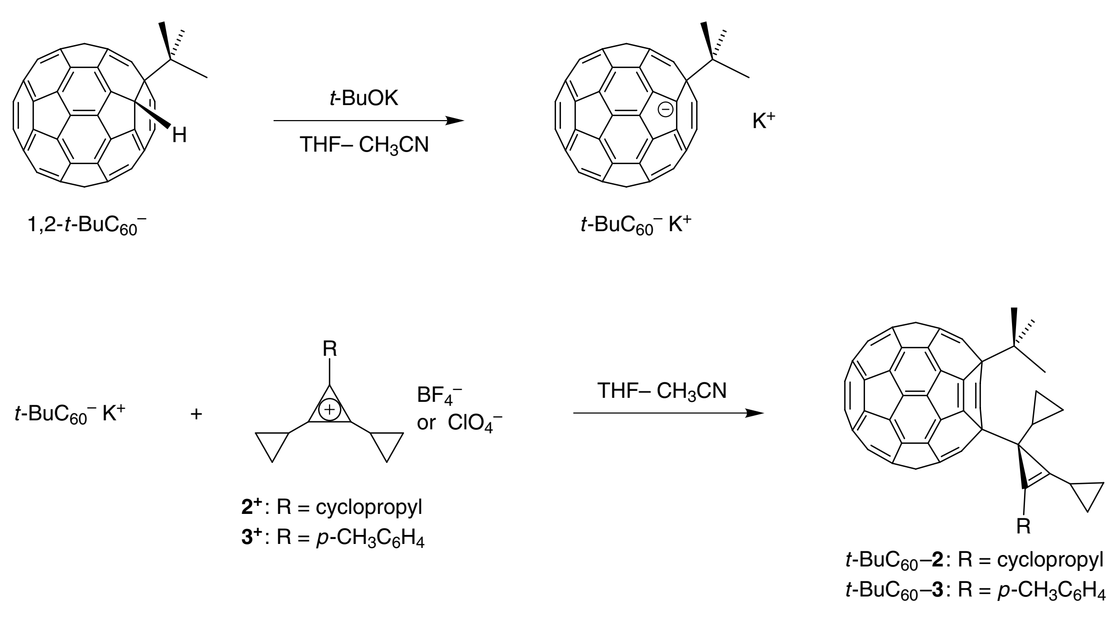

Scheme 3.

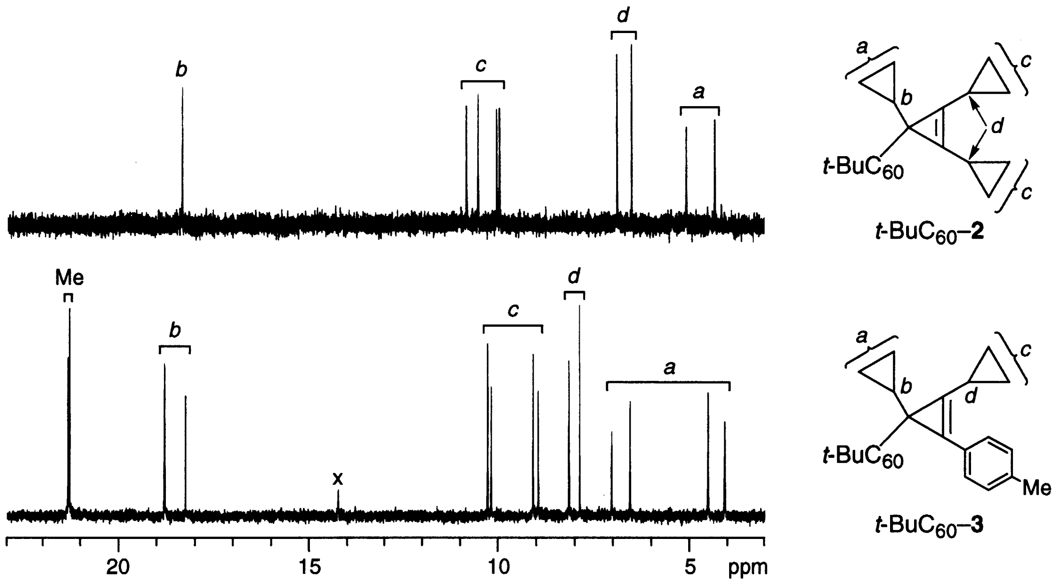

Figure 1. ^{13}C NMR spectra (100 MHz, CS_2–$CDCl_3$ 2:1) of t-BuC$_{60}$-**2** and t-BuC$_{60}$-**3** (mixture of diastereomers, 55:45). The assignments of peaks are based on DEPT and H–C COSY measurements. ×: impurity.

The above results suggest that the formation of the 1,4-adduct is also favored in the reaction of $\mathbf{3}^+$ with t-BuC$_{60}^-$. Three structures, A–C, are possible for t-BuC$_{60}$-**3** (Scheme 4), in which the p-tolyl group is bound to different positions. The obtained product, however, contained only two isomers (molar ratio 55:45), as evidenced by the ^{1}H NMR spectra of the product mixture, which showed two sets of p-tolyl signals. In accord with the expected formation of two 1,4-isomers, the ^{13}C NMR spectrum showed 112 aromatic/olefinic and 24 aliphatic signals (theor. 128 and 24 signals, respectively). The two isomers were assigned to a pair of diastereomers A and B, since for each isomer one methine carbon out of two is significantly deshielded (δ 18.8 and 18.3; Fig. 1) compared to the other (δ 8.2 and 7.9). A possible reason for the absence of isomer C is the steric hindrance of the phenyl ring. The separation of isomers A and B could not be achieved, due to high tendency toward heterolytic C–C bond cleavage (vide infra) during chromatographic separation, resulting in the formation of t-BuC$_{60}$H.

The ^{1}H NOE difference spectra for t-BuC$_{60}$-**2** and t-BuC$_{60}$-**3**, which indicated that the cyclopropyl groups are close to the *tert*-butyl group, strongly support the proposed 1,4-adduct structures—irradiation of the *tert*-butyl protons caused a significant enhancement (17–29%) of the methine-proton signals. The broad absorption at 442–446 nm observed in the UV/Vis spectra (in cyclohexane) is also typical of 1,4-adducts.[15,21]

2.2. Redox potentials of disubstituted dihydro[60]-fullerenes

Cyclic voltammetry of the 1,4-adducts t-BuC$_{60}$-**2** and t-BuC$_{60}$-**3** exhibited three reversible reduction waves and an irreversible oxidation wave. The reduction waves are, consistent with the high LUMO levels, 0.15–0.26 V more negative than those of parent C_{60} (Table 1). The $E_{\mathrm{red}}(1)$ and $E_{\mathrm{red}}(2)$ of a series of 1,4-adducts, including tropylium ion adducts t-BuC$_{60}$-**1**, are correlated with the LUMO energy levels in a linear fashion, and the $E_{\mathrm{red}}(3)$ is correlated with LUMO+1 (Fig. 2).[22] The relatively low sensitivity of the reduction potentials compared to the MO levels in the sense

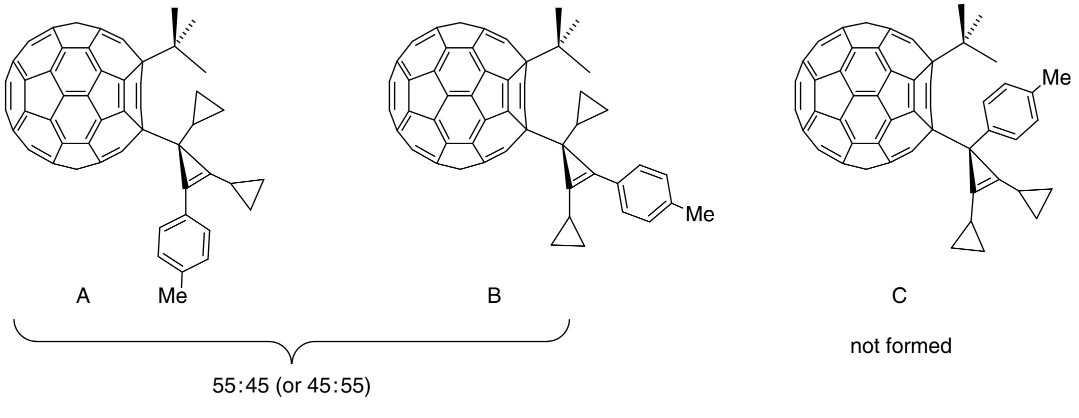

Scheme 4.

Table 1. CV redox potentials and MO energy levels

Compound	Redox potential (V vs Fc/Fc$^+$)[a]				MO energy level (eV)[b]	
	E_{ox}[c]	$E_{red}(1)$[d]	$E_{red}(2)$[d]	$E_{red}(3)$[d]	LUMO	LUMO+1
C_{60}	1.37	−1.09	−1.48	−1.93	−2.89	−2.89
t-BuC_{60}-**2**[e]	1.49	−1.28	−1.63	−2.18	−2.67	−2.63
t-BuC_{60}-**3**[e,f]	1.58	−1.28	−1.64	−2.19	−2.66[g]	−2.62[g]

[a] Half-wave potentials. Peak potentials are shown for irreversible waves. Solvent, 1,2-dichlorobenzene; supporting electrolyte, 0.1 M $Bu_4N^+PF_6^-$; scan rate, 20 mV/s.

[b] Calculated by the PM3 method.

[c] Irreversible.

[d] Reversible.

[e] An irreversible oxidation wave at −0.67 V and a reversible reduction wave at −1.99 V due to *t*-BuC_{60}^- were also observed.

[f] Mixture of diastereomers (Scheme 4, A and B, 55:45 or 45:55).

[g] Isomers A and B have essentially the same LUMO and LUMO+1 levels.

of free energy can be attributed to ion pairing or the solvation of reduced species in solution.

The voltammograms of *t*-BuC_{60}-**2** and *t*-BuC_{60}-**3** showed an additional reversible wave at −1.99 V and an irreversible oxidation wave at −0.67 V. As proposed earlier,[15] these redox waves can be attributed to *t*-BuC_{60}^- which is formed by C–C bond cleavage during the initial reduction processes, since these waves increased in intensity in the presence of added base. Furthermore, the *t*-BuC_{60}^-, generated by deprotonation of 1,2-*t*-BuC_{60}H by *t*-BuOK, also showed reduction and oxidation waves at the same potentials.

2.3. Inertness of *t*-BuC_{60}^- and 4^+ toward one another

2.3.1. Electrical conductivity of the mixture of *t*-Bu$C_{60}^-K^+$ and $4^+ClO_4^-$ in solution. Typically a carbocation and a carbanion do not coexist because of the high reactivity of the ions toward coordination to form a carbon–carbon covalent bond. Carbocation–carbanion salts, however, have been isolated in several exceptional cases, using cationic and/or anionic moieties that are stabilized by strongly electron-donating or electron-withdrawing substituents containing heteroatoms.[23] In addition, we have reported that carbocation–carbanion salts can also be constructed from hydrocarbon components.[11,13] Thus, resonance-stabilized anion $\mathbf{6}^-$ does not react with $\mathbf{2}^+$, $\mathbf{3}^+$, or $\mathbf{4}^+$, but, rather, forms hydrocarbon salts $\mathbf{2}^+\mathbf{6}^-$,[11e,g] $\mathbf{3}^+\mathbf{6}^-$,[11c,d] and $\mathbf{4}^+\mathbf{6}^-$.[11e,h] The salts $\mathbf{2}^+\mathbf{6}^-$ and $\mathbf{4}^+\mathbf{6}^-$ were found to behave as strong electrolytes in DMSO.

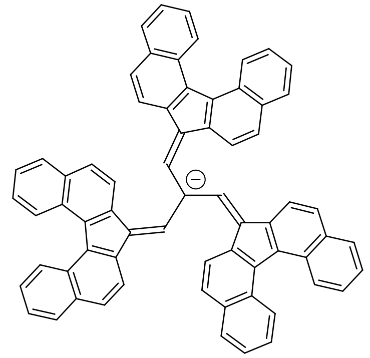

$\mathbf{6}^-$

As expected from the high thermodynamic stability of tris[1-(5-isopropyl-3,8-dimethylazulenyl)]cyclopropenylium ion $\mathbf{4}^+$ (pK_{R^+} 13.6[19b]), the Vis–NIR spectra of the mixture of *t*-Bu$C_{60}^-K^+$ and $\mathbf{4}^+ClO_4^-$ showed that *t*-BuC_{60}^- can coexist with $\mathbf{4}^+$ in DMSO solution. Conductivity measurements also indicated that no carbon–carbon coordination occurred when *t*-Bu$C_{60}^-K^+$ and $\mathbf{4}^+ClO_4^-$ were placed together in DMSO. The molar conductivities (Λ) of DMSO solutions containing *t*-Bu$C_{60}^-K^+$ and $\mathbf{4}^+ClO_4^-$ at a constant molar ratio (1.27:1) showed a linear dependence against the square root of concentration, indicating that the mixed salt is a strong electrolyte.[24] By extrapolating the

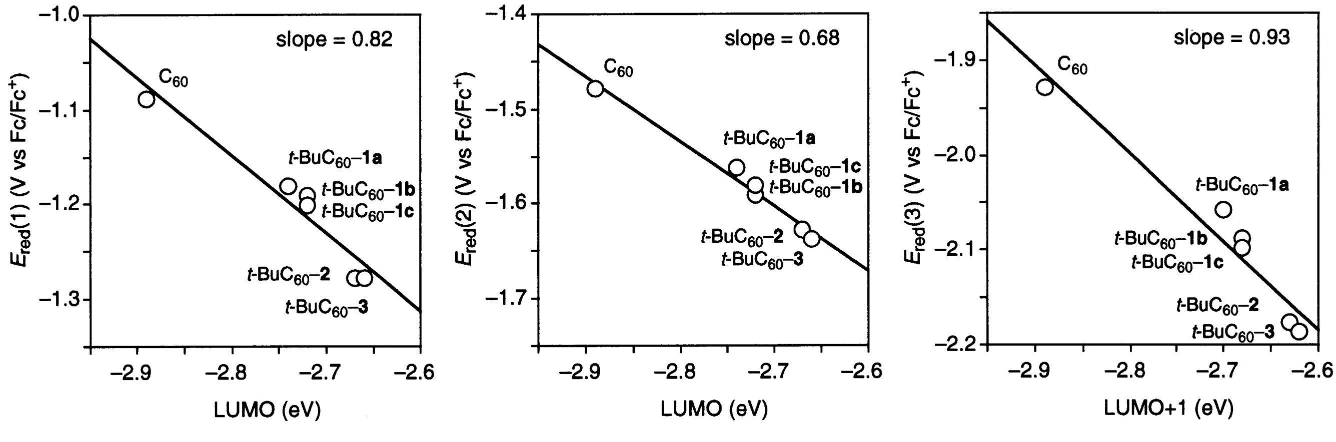

Figure 2. Plots of reduction potentials vs MO energy levels calculated by the PM3 method. The potentials for C_{60} and *t*-BuC_{60}-**1** were taken from Ref. 15.

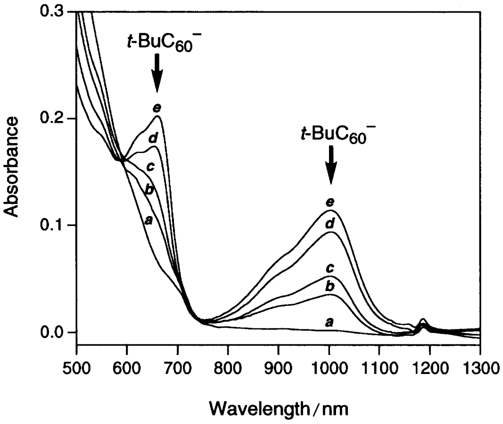

Figure 3. , Visible/near-IR absorption spectra of t-BuC$_{60}$-**3** (mixture of diastereomers 55:45) in equilibrium with its ionized form in degassed DMSO–THF. Cell length, 1 cm. Mole fraction of DMSO (initial concentration/M): (a) 0.015 (15.3×10^{-5}); (b) 0.056 (22.9×10^{-5}); (c) 0.221 (15.3×10^{-5}); (d) 0.532 (11.9×10^{-5}); (e) 0.820 (9.83×10^{-5}).

plot to infinite dilution, the limiting molar conductivity (Λ_0) for [t-BuC$_{60}^-$K$^+$]$_{1.27}$[**4**$^+$ClO$_4^-$] was determined to be 59.4 S cm^2/mol.

In order to verify the absence of coordination between the ions, similar measurements were carried out for t-BuC$_{60}^-$K$^+$ alone, resulting in a linear Λ–$c^{1/2}$ plot, which gave a Λ_0 of 25.7 S cm^2/mol. From this value and the reported Λ_0 of **4**$^+$ClO$_4^-$ (30.2 S cm^2/mol),[11e] a Λ_0 of 62.8 S cm^2/mol (25.7×1.27+30.2) is obtained as the sum of the contributions of the component ions which exist in completely ionized form. The fairly good agreement between this value and the experimentally observed Λ_0 of 59.4 S cm^2/mol indicates that t-BuC$_{60}^-$ and **4**$^+$ exist as such in dilute DMSO solution.[25]

2.3.2. Isolation of the hydrocarbon salt 4$^+$$t$-BuC$_{60}^-$.

The result of electrical conductivity measurements led to the isolation of the salt of **4**$^+$ and t-BuC$_{60}^-$ as a pure hydrocarbon solid. To prepare the salt, a THF solution of **4**$^+$ClO$_4^-$ was mixed with an equimolar amount of t-BuC$_{60}^-$K$^+$ in THF under a stream of argon. The addition of CH$_3$CN to the mixture resulted in the precipitation of a hydrocarbon, while the inorganic component, KClO$_4$, remained in solution. The precipitate was isolated as a dark, reddish-brown powder by filtration.

The salt structure of the powder is supported by IR and Vis–NIR spectra of KBr disks, which showed absorptions corresponding to **4**$^+$ and t-BuC$_{60}^-$.[26] However, no sharp lines were observed in powder X-ray diffraction (CuKα radiation), indicating that only a very low degree of order exists in the obtained solid. The visible/near-IR absorption of a solution in DMSO–THF (4:1 v/v) had maxima at 656sh and 995 nm (molar absorptivity 5260 and 2420, respectively), and agreed with the independently measured absorption of t-BuC$_{60}^-$, superimposed with that of **4**$^+$. This result, which is in agreement with the electrical conductivity measurements, indicates that dissolution occurs without carbon–carbon coordination or tight ion-pair formation. The ^{1}H NMR spectrum, obtained in THF-d_8, also showed quantitative ionization, but the signals corresponding to **4**$^+$ and t-BuC$_{60}^-$ simultaneously disappeared in 16 h with the concomitant formation of a mixture of unidentified compounds.[26]

2.4. Heterolysis of t-BuC$_{60}$-2 and t-BuC$_{60}$-3

Although the somewhat less stabilized carbocations **2**$^+$ and **3**$^+$ did not give salts with t-BuC$_{60}^-$ but formed a C–C covalent bond, the hydrocarbons obtained by those reactions, t-BuC$_{60}$-**2** and t-BuC$_{60}$-**3**, were found to undergo heterolysis of the C–C bond, as a result of the high stabilities of the component ions. When dissolved in mixtures of DMSO–THF or DMSO–CS$_2$, these molecules partially dissociated into the original ions, t-BuC$_{60}^-$ and **2**$^+$ or **3**$^+$, giving rise to a greenish colored solution (Fig. 3, λ_{max} 656 and 995 nm), which is indicative of the formation of t-BuC$_{60}^-$. Furthermore, the ^{1}H NMR spectrum of t-BuC$_{60}$-**2** in DMSO-d_6–THF-d_8 (1:1 v/v), which showed the formation of t-BuC$_{60}^-$ and **2**$^+$ coexisting with unchanged t-BuC$_{60}$-**2**, serves as a direct demonstration of reversible dissociation. In contrast, no dissociation was detected in

Table 2. Thermodynamic parameters for the heterolysis of t-BuC$_{60}$-**2** and t-BuC$_{60}$-**3** in DMSO–THF mixed solvents at 25°C

Compound	Mole fraction of DMSO	Dielectric constant[a]	Initial concentration (10^{-5} M)	Degree of dissociation[b]	$\Delta G°_{het}$ (kcal/mol)
t-BuC$_{60}$-**2**	0.000	7.5	5.92	0.010	11.2
	0.006	7.7	4.72	0.034	9.9
	0.011	7.9	5.34	0.065	9.0
	0.023	8.2	3.90	0.142	8.2
	0.056	9.4	9.63	0.284	6.8
	0.221	15.3	7.89	0.608	5.6
	0.532	27.0	12.1	0.738	4.9
	0.820	38.7	11.6	0.759	4.9
t-BuC$_{60}$-**3**	0.014	7.9	36.3	0.0004	13.9
	0.015	8.0	15.3	0.003	12.0
	0.017	8.0	11.7	0.011	10.7
	0.023	8.2	6.13	0.032	9.8
	0.056	9.4	22.9	0.058	8.3
	0.221	15.3	15.3	0.135	7.5
	0.532	27.0	11.9	0.307	6.5
	0.820	38.7	9.83	0.450	6.1

[a] Calculated from the equation $\epsilon=7.47+34.08x+4.93x^2$ (x: mole fraction of DMSO); see Section 4.

[b] Determined from the concentration of t-BuC$_{60}^-$ (λ_{max} 995 nm, molar absorptivity 2400) with an averaged experimental error ±0.001.

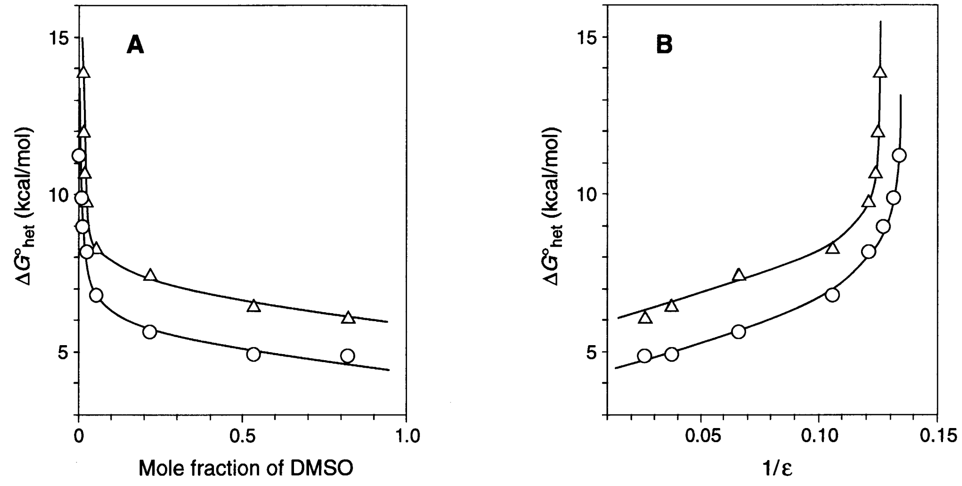

Figure 4. Free energy of heterolysis ($\Delta G°_{het}$) for *t*-BuC_{60}-**2** (○) and *t*-BuC_{60}-**3** (△) in DMSO–THF mixed solvents at 25°C. (A) $\Delta G°_{het}$ vs mole fraction of DMSO. (B) $\Delta G°_{het}$ vs reciprocal of solvent dielectric constant.

nonpolar solvents such as cyclohexane and CS_2.

$$t\text{-BuC}_{60}\text{-}\mathbf{2} \rightleftharpoons t\text{-BuC}_{60}^{-} + \mathbf{2}^{+}$$

$$t\text{-BuC}_{60}\text{-}\mathbf{3} \rightleftharpoons t\text{-BuC}_{60}^{-} + \mathbf{3}^{+}$$

It has been reported by us[11e] and by Arnett et al.[12b] that, although the free energy of heterolysis, $\Delta G°_{het}$, of a C–C covalent bond in solution correlates linearly with the reciprocal of the solvent dielectric constant in accordance with the Born equation, a deviation from this linear relationship is observed for basic coordinating solvents such as DMSO. To investigate the influence of the electron-pair donating effect of DMSO on the present system, the dissociation in DMSO–THF binary solvents was studied. Table 2 lists the observed degree of ionic dissociation, determined from the absorbance at λ_{max} 995 nm (molar absorptivity 2400[19b]), and $\Delta G°_{het}$ derived therefrom. As can be seen in Fig. 4A, a large decrease in $\Delta G°_{het}$ occurred when small amounts of DMSO were added to pure THF, while this decrease became more gradual for mole fractions of DMSO greater than 0.05. The non-dielectric behavior of the heterolysis is demonstrated by the curved $\Delta G°_{het}$–$1/\epsilon$ plot (Fig. 4B), which indicates that the heterolysis is controlled by, in addition to the bulk polarity of the solvent, the preferential solvation of ions by DMSO. In particular, the large donor number of DMSO (29.8)[27] suggests a Lewis base-type coordination of the sulfoxide oxygen to the carbocation (Scheme 5). The development of such an interaction would effectively enhance ionization by small amounts of added DMSO, but, after the coordination is completed, a linear Born plot would be established, as can be seen in the region $1/\epsilon<0.11$ of Fig. 4B.

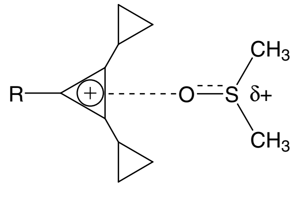

R = cyclopropyl or *p*-$CH_3C_6H_4$

Scheme 5.

The degree of dissociation was also determined in DMSO–CS_2 (4:1 v/v) (Table 3), for comparison of the data with those reported for tropylium ion adducts *t*-BuC_{60}-**1**.[14,15] It is noteworthy that the heterolysis of *t*-BuC_{60}-**2** was essentially complete (>99%), indicating that $\Delta G°_{het}$ is smaller than 3 kcal/mol. In this context, Arnett et al. have established an empirical relationship for the heterolysis of C–C bond which forms a tertiary carbocation, $\Delta H_{het}=8.895-0.648(pK_{R^+})+1.294(pK_{HA})$, where pK_{HA} is the pK_a of the conjugate acid of the carbanion.[28] By this equation, the ΔH_{het}s for *t*-BuC_{60}-**2** and *t*-BuC_{60}-**3** are predicted to be 9.8 and 11.5 kcal/mol, respectively. If one assumes that the $\Delta S°_{het}$ is ca. −20 cal/(mol K), as we have reported for the heterolysis of hydrocarbons containing $\mathbf{6}^-$ as the anionic moiety,[11c] the $\Delta G°_{het}$s are estimated to be 16–18 kcal/mol for the present compounds. The large difference between this value and the observed $\Delta G°_{het}$s in Table 3 can be explained by steric repulsion of the large groups attached to C_{60} and solvation of the cyclopropenylium ion by DMSO. Although rather poor, a linear free-energy relationship was found between $\Delta G°_{het}$ and the pK_{R^+} of the cationic component (Fig. 5). This result is somewhat unexpected, since the steric effects of the substituents around the cationic centers of **1a–c**$^+$, **2**$^+$, and **3**$^+$ are significantly different.[29] Probably, the drop in $\Delta G°_{het}$, due to

Table 3. Thermodynamic parameters for the heterolysis of *t*-BuC_{60}-**2** and *t*-BuC_{60}-**3** in DMSO–CS_2 (4:1 v/v) at 25°C

Compound	Initial concentration (10^{-5} M)	Degree of dissociation[a]	$\Delta G°_{het}$ (kcal/mol)
t-BuC_{60}-**2**	5.7–10.3	>0.99	<3
t-BuC_{60}-**3**	10.3	0.41	6.2

[a] Determined from the concentration of *t*-BuC_{60}^- (λ_{max} 995 nm, molar absorptivity 2400).

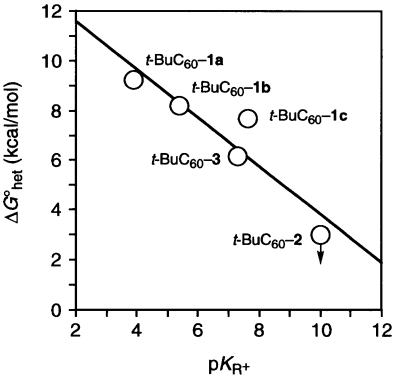

Figure 5. Plot of the free energy of heterolysis in DMSO–CS_2 (4:1 v/v) for hydrocarbons *t*-BuC_{60}-R vs pK_{R^+} of R^+ in 50% aq. CH_3CN at 25°C. The free energies for *t*-BuC_{60}-**1** have been reported previously (Ref. 15). The pK_{R^+} values were taken from the literature (Refs. 11c, 16b, 18b, 19b).

weakening of the C–C bond by the bulkiness of the cationic moiety, is partially canceled by the hindered solvation of the carbocation.

2.5. Reaction of *t*-BuC_{60}^- with 5^+

In order to test the importance of the steric effect, the reaction of *t*-BuC_{60}^- with bulky cation $\mathbf{5}^+$ was carried out. Cation $\mathbf{5}^+$ has a pK_{R^+} of 6.5,[18b] indicating that the thermodynamic stability of this cation, as estimated by its reactivity toward water, is lower than $\mathbf{2}^+$ and $\mathbf{3}^+$ by at least 0.7 p*K* units. From the $\Delta G^\circ_{het}-pK_{R^+}$ relationship shown in Fig. 5, one would expect that coordination would occur between *t*-BuC_{60}^- and $\mathbf{5}^+$. If this is the case, the excessive steric effect may result in regioisomers other than 1,2- and 1,4-adducts in which the cyclopropenyl group is more distant from the *tert*-butyl group on the C_{60} sphere. Examples of such cases include the formation of 1,16-disilyl adducts by the reaction of C_{60} with silyllithiums and disilanes.[30]

When THF solutions of *t*-$BuC_{60}^-K^+$ and $\mathbf{5}^+ClO_4^-$ were mixed under an argon atmosphere, the dark green color of *t*-BuC_{60}^- immediately disappeared. NMR analysis indicated the formation of hydrolysis products, *t*-$BuC_{60}H$ (1,2- and 1,4-isomers)[31] and ether **7**, due to a trace amount of water, rather than C–C coordination products.

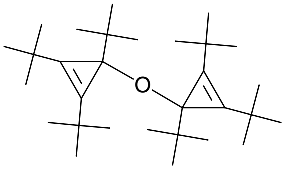

7

In order to determine the course of the reaction in the absence of water, the reaction was carried out in a vessel predried by a vacuum line ($<10^{-4}$ Torr), and the dark green color of *t*-BuC_{60}^- persisted in this case. NMR analysis of the vacuum-sealed solution indicated that the product consists of *t*-BuC_{60}^-, $\mathbf{5}^+$, 1,2-*t*-$BuC_{60}H$, and **7** in a molar ratio of 1.00:1.13:0.51:0.25 (Fig. 6). The coexistence of $\mathbf{5}^+$ and *t*-BuC_{60}^-, and the absence of coordination products indicate that steric hindrance suppressed the coordination between the ions. This result is not surprising, considering that the coordination would be severely hindered because of repulsion between the *tert*-butyl groups of $\mathbf{5}^+$ and the π-electron cloud of the C_{60} sphere. The isolation of the hydrocarbon salt $\mathbf{5}^+$*t*-BuC_{60}^-, however, was not successful because of its high sensitivity to moisture, leading to the formation of *t*-$BuC_{60}H$ and **7**.

3. Conclusion

Carbon–carbon covalent bond formation is one of the most commonly observed reactions between a carbocation and a carbanion. This study demonstrates how the reactivity between *t*-BuC_{60}^- and substituted cyclopropenylium ions toward C–C coordination changes, depending on thermodynamic stability and steric crowding of the cation. A highly stabilized carbocation $\mathbf{4}^+$ did not react with *t*-BuC_{60}^- and gave a salt, which behaves as a strong electrolyte in solution. The less stable cations, $\mathbf{2}^+$ and $\mathbf{3}^+$, gave covalent hydrocarbons, which contain a C–C bond capable of undergoing heterolysis in polar media. The degree of dissociation ranged between zero (in $CHCl_3$) and 100% (in DMSO–CS_2 4:1 v/v) by changing the solvent, thus enabling us to precisely determine the dissociation constant over a wide range of solvent polarity. The result of the reaction between

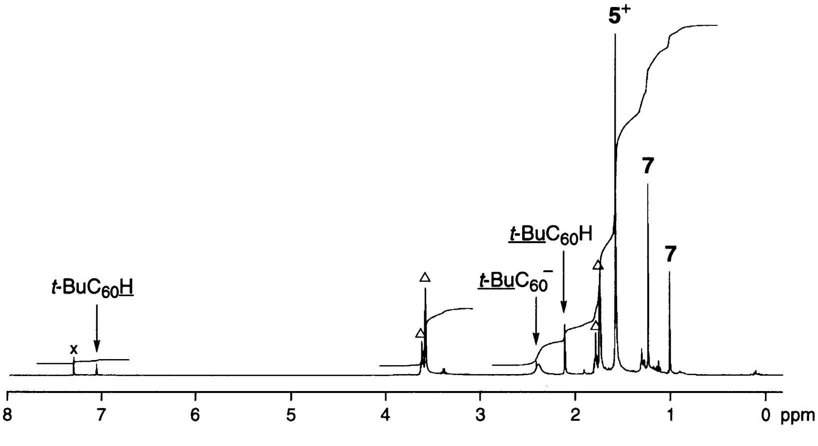

Figure 6. ^1H NMR spectrum (400 MHz, THF-d_8) of the product mixture from the reaction of *t*-BuC_{60}^- with $\mathbf{5}^+$ in THF at ambient temperature. △: solvent. ×: $CHCl_3$ (contaminant from the vacuum line).

t-BuC_{60}^{-} and $\mathbf{5}^{+}$ indicates that steric hindrance effectively suppresses carbocation–carbanion coordination, but that the intrinsically high reactivity of the cation can be a driving force for the simultaneous collapse of both ions by trace amounts of water.

4. Experimental

4.1. General procedures

IR and visible/near-IR spectra were recorded on a Perkin–Elmer model 1600 and JASCO V-570 spectrophotometers, respectively. FAB mass spectra were obtained on a JEOL JMS-HX110 mass spectrometer in the negative ion mode using *o*-nitrophenyl octyl ether as a matrix. PM3 calculations[32] were carried out using the MOPAC package on an IBM RS/6000 computer. Elemental analyses were performed by the Microanalytical Center, Kyoto University. ^{1}H and ^{13}C NMR spectra were obtained with a JEOL EX400 (^{1}H, 400 MHz; ^{13}C, 100 MHz) instrument. Peak assignments are based on DEPT, COSY, and H–C COSY measurements. For the ^{13}C NMR spectra of t-BuC_{60}-**2** and t-BuC_{60}-**3**, free induction decays were collected using 128K data points, and the accumulated data were processed after zero-filling to 1024K with no window function. ^{1}H NOEs were determined by the gated decoupling method using degassed solutions of t-BuC_{60}-**2** and t-BuC_{60}-**3** in CS_2–$CDCl_3$ (2:1). A saturation period of 8 s was taken before each pulse.

4.2. Materials

Reagents were of reagent-grade quality except where otherwise noted. Tetrahydrofuran was distilled from sodium benzophenone ketyl prior to use. DMSO was dried over 4 A molecular sieves for at least 1 day, and then distilled over CaH_2. Acetonitrile was distilled over P_2O_5. *tert*-Butyl-1,2-dihydro[60]fullerene (1,2-t-$BuC_{60}H$) was prepared as described previously.[15,20] Cyclopropenylium ion salts ($\mathbf{2}^{+}BF_4^{-}$,[16] $\mathbf{3}^{+}ClO_4^{-}$,[11c] $\mathbf{4}^{+}ClO_4^{-}$,[17] and $\mathbf{5}^{+}ClO_4^{-}$[18]) were synthesized by methods described in the literature.

4.2.1. 1-*tert*-Butyl-4-(tricyclopropyl-2-cyclopropen-1-yl)-1,4-dihydro[60]fullerene (*t*-BuC$_{60}$-2). To a THF solution (20 mL) of 1,2-t-$BuC_{60}H$ (19.3 mg, 24.8 μmol) was added a 10% excess of t-BuOK in THF (20 mM) under argon, in the dark, at room temperature, and the mixture was stirred for 30 min. To the resulting dark green solution of t-$BuC_{60}^{-}K^{+}$ was added a THF–acetonitrile solution (4:1 v/v, 10 mL) of $\mathbf{2}^{+}BF_4^{-}$ (6.70 mg, 27.2 μmol). The mixture was stirred for 15 min, and the solvent removed by flash evaporation. The dark brown residue was dissolved in CS_2 and filtered through a 0.45 μm Teflon membrane filter to remove KBF_4 and unchanged $\mathbf{2}^{+}BF_4^{-}$. The CS_2 was evaporated to give t-BuC_{60}-**2** as a dark brown solid (23.1 mg, 100%). This solid was essentially pure by NMR spectra. Further purification of this solid by chromatography on silica gel was unsuccessful owing to its rapid decomposition in the column. All analyses and heterolysis measurements were carried out without further purification of the compound. ^{1}H NMR (CS_2–$CDCl_3$ 2:1) δ 2.13–2.03 (m, 1H), 1.94 (s, 9H), 1.80–1.71 (m, 1H), 1.71–1.62 (m, 1H), 1.04–0.89 (m, 4H), 0.71–0.55 (m, 6H), 0.55–0.48 (m, 1H), 0.43–0.35 (m, 1H); ^{13}C NMR (CS_2–$CDCl_3$ 2:1) δ 27.90 (CH_3); 10.85, 10.54, 10.05, 9.98, 5.10, 4.35 (CH_2); 18.38, 6.91, 6.52 (CH); 160.35, 157.62, 152.79, 151.04, 149.93, 149.47, 148.33, 148.27, 148.20, 147.89, 147.22, 146.86, 146.80, 146.64, 146.61, 146.58, 146.49, 145.75, 145.21 (2C); 145.06, 144.76, 144.70, 144.62, 144.61, 144.54, 144.26, 144.16, 144.13, 144.08, 144.00, 143.98, 143.88, 143.799, 143.794, 143.72, 143.34, 143.12, 142.98, 142.88, 142.84, 142.79, 142.71, 142.70, 142.61, 142.47, 142.45, 142.36, 142.32, 142.27, 141.98, 141.80, 141.17, 140.00, 139.12, 138.58, 138.07, 135.69, 117.75, 117.15, 68.06, 67.66, 42.40, 40.55 (C); IR (KBr) 2959, 1460, 1426, 1365, 1188, 1016, 757, 526; UV/Vis (cyclohexane) λ_{max} (ϵ) 213 (131 000), 257 (101 000), 327sh (29 900), 446 (5920) with end absorption to 750 nm; FAB MS *m/z* 936 (M), 879 (M−t-Bu), 777 (t-BuC_{60}), 720 (C_{60}).

4.2.2. 1-*tert*-Butyl-4-[1,2-dicyclopropyl-3-(*p*-methylphenyl)-2-cyclopropen-1-yl]-1,4-dihydro[60]fullerene (*t*-BuC$_{60}$-3). This compound was synthesized by the above-described method using 18.4 mg (23.6 μmol) of 1,2-t-$BuC_{60}H$ and 8.17 mg (26.5 μmol) of $\mathbf{3}^{+}ClO_4^{-}$. Dark brown solid; yield 99%. As NMR data showed, the obtained product contained two isomers (Scheme 4, isomers A and B, molar ratio 55:45 or 45:55). In the NMR data below, signals marked with * and † are those of the major and minor isomers, respectively. ^{1}H NMR (CS_2–$CDCl_3$ 2:1) δ $7.22^{\dagger}$ (d, J=8.1 Hz), 7.18^{*} (d, J=8.1 Hz), $7.02^{\dagger}$ (d, J=8.1 Hz), 6.98^{*} (d, J=8.1 Hz), 2.4–1.85 (m), $2.30^{\dagger}$ (s), 2.27^{*} (s), 1.96^{*} (s), $1.95^{\dagger}$ (s), 1.2–0.5 (m), 0.31–0.17 (m); ^{13}C NMR (CS_2–$CDCl_3$ 2:1) δ $28.11^{\dagger}$, 28.08^{*}, $21.34^{\dagger}$, 21.31^{*} (CH_3); 10.28^{*}, $10.18^{\dagger}$, 9.10^{*}, $8.97^{\dagger}$, $7.05^{\dagger}$, 6.57^{*}, 4.52^{*}, $4.08^{\dagger}$ (CH_2); 129.18, 129.04, 129.03, 129.00, 18.80^{*}, $18.27^{\dagger}$, $8.17^{\dagger}$, 7.89^{*} (CH); 160.75, 160.42, 157.62, 157.51, 152.77, 152.43, 151.52, 150.71, 150.15, 149.85, 149.46, 149.31, 148.37, 148.29, 148.23, 148.20, 148.01, 147.94, 147.88, 147.75, 147.06, 146.88, 146.85, 146.77, 146.73, 146.651, 146.646, 146.62, 146.59, 146.57, 146.55, 146.47, 145.96, 145.70, 145.63, 145.25, 145.20, 145.19, 145.15, 144.85, 144.80, 144.73, 144.61, 144.583, 144.576, 144.44, 144.34, 144.20, 144.14, 144.13, 144.11, 144.10, 144.06, 144.05, 144.04, 144.02, 143.98, 143.92, 143.87, 143.83, 143.82, 143.81, 143.78, 143.75, 143.73, 143.35, 143.26, 143.24, 143.19, 143.11, 143.10, 143.00, 142.91, 142.87, 142.86, 142.85, 142.84, 142.83, 142.82, 142.81, 142.78, 142.75, 142.63, 142.62, 142.53, 142.50, 142.41, 142.353, 142.348, 142.341, 142.337, 142.332, 142.30, 142.24, 142.14, 142.07, 141.92, 141.82, 141.19, 141.10, 139.96, 139.94, 139.11, 139.08, 138.69, 138.61, 138.15, 137.75, 137.50, 137.49, 136.41, 134.54, 125.52, 125.46, 125.26, 123.02, 112.40, 112.03, $68.10^{\dagger}$, 68.06^{*}, $67.55^{\dagger}$, 67.45^{*}, $42.52^{\dagger}$, 42.10^{*}, $40.69^{\dagger}$, 40.42^{*} (C); IR (KBr) 2918, 1508, 1459, 1426, 1364, 1188, 1016, 816, 526; UV/Vis (cyclohexane) λ_{max} (ϵ) 211 (114 000), 257 (83 500), 327sh (25 200), 442 (6060) with end absorption to 750 nm; FAB MS *m/z* 986 (M), 929 (M−t-Bu), 777 (t-BuC_{60}), 720 (C_{60}).

4.2.3. Hydrocarbon salt $\mathbf{4}^{+}t$-$\mathbf{BuC_{60}}^{-}$. To a stirred suspension of 1,2-t-$BuC_{60}H$ (6.11 mg, 7.85 μmol) in THF (2.5 mL) was added an equimolar amount of t-BuOK in THF (0.016 M) under argon at room temperature. After 15 min, a THF solution (3.0 mL) of $\mathbf{4}^{+}ClO_4^{-}$ (5.70 mg, 7.84 μmol) was added. The solvent was quickly evaporated in vacuo to give a reddish-brown solid. The solid was dissolved in THF (0.8 mL) and reprecipitated by adding CH_3CN (5 mL) under argon. After centrifugation, the supernatant solution, which contained $KClO_4$, was separated from the precipitate. The precipitate was washed three times with a small amount of CH_3CN under argon and vacuum dried to give a dark reddish-brown powder (4.5 mg, 41%).[26] Elemental analyses showed that the carbon and hydrogen contents decreased rapidly on exposure to air, while the C/H percent ratio remained constant at the theoretical value of $C_{48}H_{51}{}^{+}\cdot C_{64}H_9{}^{-}$. Calcd for $C_{112}H_{60}$: C, 95.70; H, 4.30. Found: C, 91.71; H, 4.12 (immediately after preparation). C, 87.91; H, 3.86 (after exposure to air for 30 min).

4.2.4. Bis(1,2,3-tri-*tert*-butyl-2-cyclopropen-1-yl) ether (7). Ether **7** has been reported as a precursor for the synthesis of $\mathbf{5}^{+}ClO_4{}^{-}$ and has a characteristic cyclopropene absorption at 1825 cm^{-1}.[18b] In the present study, this unstable ether was prepared in order to obtain the ^1H NMR data, required for product identification. A CH_3CN solution (10 mL) of $\mathbf{5}^{+}ClO_4{}^{-}$ (10.8 mg) was diluted with 10 mL of aqueous sodium tetraborate buffer (0.01 M, pH 9.2). After 10 min, the hydrolysis product was extracted with CH_2Cl_2 (15 mL), and the solvent was evaporated. The residual colorless oil was dissolved in 1 mL of $CDCl_3$, and the solution was subjected to ^1H NMR analysis: δ 1.22 (s, 36H), 0.99 (s, 18H).

4.3. Reaction of *t*-BuC$_{60}{}^{-}$ with 5^{+}

4.3.1. Reaction under argon atmosphere. The reaction was carried out in a manner similar to that described for the synthesis of *t*-BuC$_{60}$-**2** using 4.44 mg (5.70 μmol) of 1,2-*t*-BuC$_{60}$H and 2.01 mg (6.55 μmol) of $\mathbf{5}^{+}ClO_4{}^{-}$. NMR analysis of the resulting dark brown solid (5.0 mg) indicated that *t*-BuC$_{60}$H (1,2- and 1,4-isomers, 66:34) and **7** were the only products. The observed chemical shifts of 1,2-*t*-BuC$_{60}$H (δ 6.65 and 2.06) and 1,4-*t*-BuC$_{60}$H (δ 6.29 and 1.87) were in agreement with the reported values.[8,20a]

4.3.2. Reaction using a vacuum line apparatus. In a flask fitted with a side arm and an NMR sample tube, a solution of *t*-BuC$_{60}{}^{-}$K^{+} in THF (10 mL) was prepared from 1,2-*t*-BuC$_{60}$H (4.44 mg, 5.70 μmol) and 1.05 molar equivalents of *t*-BuOK. The THF was evaporated, and the flask, containing the dark green solid of *t*-BuC$_{60}{}^{-}$K^{+}, was kept at 10^{-5}–10^{-4} Torr for 3 h at room temperature for removal of water. THF (10 mL), which had been dried over sodium in another flask connected to the vacuum line, was introduced via vacuum transfer. To the resulting solution was added $\mathbf{5}^{+}ClO_4{}^{-}$ (2.16 mg, 7.04 μmol) from the side arm. The solvent was evaporated, and to the dark green residue was added THF-d_8 (1 mL), which had been dried over $LiAlH_4$, by vacuum transfer. The solution was transferred to the NMR sample tube, and the tube was sealed off under vacuum. The ^1H NMR spectrum of the solution (Fig. 6) showed that product consisted of *t*-BuC$_{60}{}^{-}$, **5**$^{+}$, 1,2-*t*-BuC$_{60}$H, and **7** in a molar ratio of 1.00:1.13:0.51:0.25. The observed chemical shifts (δ) were as follows (δ for authentic samples in THF-d_8 in parentheses): *t*-BuC$_{60}{}^{-}$, 2.38 (2.37[6]); **5**$^{+}$, 1.56 (1.56); 1,2-*t*-BuC$_{60}$H, 7.06 and 2.10 (7.05 and 2.10); **7**, 1.23 and 0.99 (1.22 and 0.99 in $CDCl_3$). As has been reported,[6] the ^1H signals of the *tert*-butyl groups in *t*-BuC$_{60}{}^{-}$ and 1,2-*t*-BuC$_{60}$H split into two signals below −90 and −30°C, respectively, owing to hindered rotation of the *tert*-butyl group.

4.4. Cyclic voltammetry

Cyclic voltammograms were recorded on a Bioanalytical System BAS CV-50W instrument. A three-electrode cell, consisting of a BAS 11-2012 glassy carbon working electrode, a Pt wire counter electrode, and an Ag/AgNO$_3$ (0.01 M in CH_3CN) reference electrode, was employed. The measurements were carried out at a scan rate of 20 mV/s for 1,2-dichlorobenzene solutions containing 1 mM of sample, 1 mM of ferrocene as an internal standard, and 0.1 M of $Bu_4N^{+}PF_6{}^{-}$ as a supporting electrolyte.

4.5. Determination of the degree of ionic dissociation of *t*-BuC$_{60}$-2 and *t*-BuC$_{60}$-3

For measurement of the degree of heterolytic dissociation of these compounds, DMSO–THF solutions of *t*-BuC$_{60}$-**2** or *t*-BuC$_{60}$-**3** (c=4–36×10^{-5} M) were prepared in a vacuum-sealed (10^{-5} Torr), 1-cm cell. The degree of ionic dissociation (α) was determined by measuring the concentration of *t*-BuC$_{60}{}^{-}$ at 25°C from the absorbance at λ_{max} 995 nm (molar absorptivity 2400). The equilibrium constant and the standard free energy of heterolysis were calculated by the equations $K_{het}=c\alpha^2/(1-\alpha)$ and $\Delta G^{\circ}_{het}=-RT\ln K_{het}$, respectively.

4.6. Electrical conductivity measurements

4.6.1. *t*-BuC$_{60}{}^{-}$K^{+} in DMSO. To a THF solution (20 mL) of 1,2-*t*-BuC$_{60}$H (8.16 mg) were added 1.05 molar equivalents of *t*-BuOK in THF (0.012 M) under argon at room temperature. Rapid removal of the solvent in vacuo gave *t*-BuC$_{60}{}^{-}$K^{+} as a dark green solid. A stock solution of *t*-BuC$_{60}{}^{-}$K^{+} in DMSO (5.24×10^{-4} M) was prepared by dissolving the *t*-BuC$_{60}{}^{-}$K^{+} in freshly degassed DMSO (20 mL). A 1.00-mL portion of the stock solution was introduced at 2 min intervals into a conductivity cell (cell constant 0.969) containing 11.00 mL of DMSO under an argon atmosphere at 25°C. Conductivity at each concentration (c), calculated by subtracting the conductivity of pure DMSO (0.17 μS/cm) from the observed value, was converted to molar conductivity, Λ. The obtained data (Λ, S cm^2/mol) are as follows [c (10^{-4} M) in parentheses]: 25.4 (1.12), 25.4 (1.40), 25.7 (1.64), 25.6 (1.85), 25.8 (2.04), 25.6 (2.21), 25.6 (2.36), 25.5 (2.50). A $\Lambda-c^{1/2}$ plot for the obtained data gave a straight line, extrapolation of which to c=0 gave a limiting molar conductivity (Λ_0) of 25.7 S cm^2/mol.

4.6.2. Mixtures of *t*-BuC$_{60}{}^{-}$K^{+} and 4^{+}ClO$_4{}^{-}$ in DMSO. A stock solution of $\mathbf{4}^{+}ClO_4{}^{-}$ in DMSO (4.12×10^{-4} M) was prepared by dissolving $\mathbf{4}^{+}ClO_4{}^{-}$ (3.55 mg) in freshly degassed DMSO (11.8 mL). Portions (0.60 mL each) of stock solutions of *t*-BuC$_{60}{}^{-}$K^{+} (5.24×10^{-4} M; see above) and of $\mathbf{4}^{+}ClO_4{}^{-}$ (4.12×10^{-4} M) were added at the same time every 2 min to a cell (cell constant 0.969), which contained 11.00 mL of DMSO under argon. The molar conductivity, Λ, was calculated for each run by dividing the observed conductivity, measured at 25°C, by the concentration of

$\mathbf{4}^+ClO_4^-$ (*c*). Since the concentration of *t*-$BuC_{60}^-K^+$ is 1.27 times that of $\mathbf{4}^+ClO_4^-$ in all runs, the Λs correspond to $[t\text{-}BuC_{60}^-K^+]_{1.27}[\mathbf{4}^+ClO_4^-]$. The obtained data ($\Lambda$, S cm^2/mol) are as follows [*c* (10^{-4} M) in parentheses]: 58.2 (0.203), 57.7 (0.508), 58.0 (0.626), 57.6 (0.727), 57.7 (0.815), 57.4 (0.892), 57.3 (0.960), 57.1 (1.02), 57.0 (1.08), 56.8 (1.12). A $\Lambda - c^{1/2}$ plot for the obtained data gave a straight line, extrapolation of which to $c=0$ gave a Λ_0 of 59.4±0.5 S cm^2/mol.

4.7. Dielectric constants

The dielectric constants of the solvents were measured at 25°C using an HP 4192A impedance analyzer over the frequency range 1.6 kHz–1 MHz. The cell consisted of two 40×10 mm^2 platinum electrodes, placed at a distance of 5 mm from each other. Satisfactory Cole plots were obtained. The data were calibrated using nitrobenzene (ϵ 34.82 at 25°C[33]) as a standard. The dielectric constants of DMSO–THF binary mixtures were determined as follows. ϵ (mole fraction of DMSO, *x*): 7.6 (0), 8.5 (0.028), 9.4 (0.057), 11.3 (0.112), 16.9 (0.276), 27.0 (0.530), 37.1 (0.774), 46.3 (1). Second-order curve fit gives an equation $\epsilon = 7.47 + 34.08x + 4.93x^2$, from which the values of dielectric constants in Table 2 were calculated.

Acknowledgements

This work was supported by the Asahi Glass Foundation, the Shorai Foundation for Science and Technology, the Watanabe Memorial Fund, and a Grant-in-Aid for Scientific Research from the Ministry of Education, Science, Sports and Culture, Japan.

References

1. (a) Reed, C. A.; Bolskar, R. D. *Chem. Rev.* **2000**, *100*, 1075–1120. (b) Hirsch, A. *The Chemistry of the Fullerenes*; Thieme: Stuttgart, 1994 (Chapter 2). See also: Kitagawa, T.; Lee, Y.; Takeuchi, K. *Chem. Commun.* **1999**, 1529–1530.
2. Niyazymbetov, M. E.; Evans, D. H.; Lerke, S. A.; Cahill, P. A.; Henderson, C. C. *J. Phys. Chem.* **1994**, *98*, 13093–13098.
3. Murata, Y.; Motoyama, K.; Komatsu, K.; Wan, T. S. M. *Tetrahedron* **1996**, *52*, 5077–5090.
4. Timmerman, P.; Anderson, H. L.; Faust, R.; Nierengarten, J. F.; Habicher, T.; Seiler, P.; Diederich, F. *Tetrahedron* **1996**, *52*, 4925–4947.
5. Keshavarz-K, M.; Knight, B.; Srdanov, G.; Wudl, F. *J. Am. Chem. Soc.* **1995**, *117*, 11371–11372.
6. Fagan, P. J.; Krusic, P. J.; Evans, D. H.; Lerke, S. A.; Johnston, E. *J. Am. Chem. Soc.* **1992**, *114*, 9697–9699.
7. It has been reported that 1,4-*t*-$BuC_{60}H$ has an even higher acidity, $5.7 < pK_a < 4.15$ (Ref. 8).
8. (a) Banim, F.; Cardin, D. J.; Heath, P. *J. Phys. Chem. Solids* **1997**, *58*, 1925–1927. (b) Banim, F.; Cardin, D. J.; Heath, P. *Chem. Commun.* **1997**, 25–26.
9. (a) Van Lier, G.; Safi, B.; Geerlings, P. *J. Chem. Soc., Perkin Trans. 2* **1998**, 349–354. (b) Van Lier, G.; Safi, B.; Geerlings, P. *J. Phys. Chem. Solids* **1997**, *58*, 1719–1727. (c) Choho, K.; Van Lier, G.; Van de Woude, G.; Geerlings, P. *J. Chem. Soc., Perkin Trans. 2* **1996**, 1723–1732.
10. (a) Miyabo, A.; Kitagawa, T.; Takeuchi, K. *J. Org. Chem.* **1993**, *58*, 2428–2435. (b) Miyabo, A.; Kitagawa, T.; Takeuchi, K. *Chem. Lett.* **1992**, 679–682.
11. (a) Kitagawa, T.; Takeuchi, K. *J. Phys. Org. Chem.* **1998**, *11*, 157–170. (b) Okamoto, K.; Takeuchi, K.; Kitagawa, T. *Adv. Phys. Org. Chem.* **1995**, *30*, 173–221. (c) Takeuchi, K.; Kitagawa, T.; Miyabo, A.; Hori, H.; Komatsu, K. *J. Org. Chem.* **1993**, *58*, 5802–5810. (d) Miyabo, A.; Takeuchi, K.; Komatsu, K.; Kitagawa, T. *Chem. Lett.* **1992**, 683–686. (e) Okamoto, K.; Kitagawa, T.; Takeuchi, K.; Komatsu, K.; Kinoshita, T.; Aonuma, S.; Nagai, M.; Miyabo, A. *J. Org. Chem.* **1990**, *55*, 996–1002. (f) Komatsu, K.; Aonuma, S.; Takeuchi, K.; Okamoto, K. *J. Org. Chem.* **1989**, *54*, 2038–2039. (g) Okamoto, K.; Kitagawa, T.; Takeuchi, K.; Komatsu, K.; Miyabo, A. *J. Chem. Soc., Chem. Commun.* **1988**, 923–924. (h) Okamoto, K.; Kitagawa, T.; Takeuchi, K.; Komatsu, K.; Takahashi, K. *J. Chem. Soc., Chem. Commun.* **1985**, 173–174.
12. Distinct observation of ionic dissociation of C–C bond was first reported by Arnett et al. for molecules containing heteroatom-substituents: Arnett, E. M.; Troughton, E. B. *Tetrahedron Lett.* **1983**, *24*, 3299–3302. See also: (a) Arnett, E. M.; Molter, K. E. *Acc. Chem. Res.* **1985**, *18*, 339–346. (b) Troughton, E. B.; Molter, K. E.; Arnett, E. M. *J. Am. Chem. Soc.* **1984**, *106*, 6726–6735. (c) Arnett, E. M.; Troughton, E. B.; McPhail, A. T.; Molter, K. E. *J. Am. Chem. Soc.* **1983**, *105*, 6172–6173.
13. Komatsu, K.; Akamatsu, H.; Aonuma, S.; Jinbu, Y.; Maekawa, N.; Takeuchi, K. *Tetrahedron* **1991**, *47*, 6951–6966.
14. Kitagawa, T.; Tanaka, T.; Takata, Y.; Takeuchi, K.; Komatsu, K. *J. Org. Chem.* **1995**, *60*, 1490–1491.
15. Kitagawa, T.; Tanaka, T.; Takata, Y.; Takeuchi, K.; Komatsu, K. *Tetrahedron* **1997**, *53*, 9965–9976.
16. (a) Moss, R. A.; Shen, S.; Krogh-Jespersen, K.; Potenza, J. A.; Schugar, H. J.; Munjal, R. C. *J. Am. Chem. Soc.* **1986**, *108*, 134–140. (b) Komatsu, K.; Tomioka, I.; Okamoto, K. *Tetrahedron Lett.* **1980**, *21*, 947–950. (c) Moss, R. A.; Munjal, R. C. *Tetrahedron Lett.* **1980**, *21*, 1221–1222.
17. Agranat, I.; Aharon-Shalom, E. *J. Org. Chem.* **1976**, *41*, 2379–2383.
18. (a) Ciabattoni, J.; Nathan, E. C.; Feiring, A. E.; Kocienski, P. J. *Org. Synth. Coll. Vol. 6*, **1988**, 991–995. (b) Ciabattoni, J.; Nathan III, E. C. *J. Am. Chem. Soc.* **1969**, *91*, 4766–4771. (c) Ciabattoni, J.; Nathan III, E. C. *J. Am. Chem. Soc.* **1968**, *90*, 4495–4496.
19. Preliminary reports of this work: (a) Kitagawa, T.; Tanaka, T.; Murakita, H.; Takeuchi, K. *J. Org. Chem.* **1999**, *64*, 2–3. (b) Tanaka, T.; Kitagawa, T.; Komatsu, K.; Takeuchi, K. *J. Am. Chem. Soc.* **1997**, *119*, 9313–9314.
20. (a) Hirsch, A.; Grösser, T.; Skiebe, A.; Soi, A. *Chem. Ber.* **1993**, *126*, 1061–1067. (b) Hirsch, A.; Soi, A.; Karfunkel, H. R. *Angew. Chem., Int. Ed. Engl.* **1992**, *31*, 766–768.
21. (a) Kadish, K. M.; Gao, X.; Van Caemelbecke, E.; Hirasaka, T.; Suenobu, T.; Fukuzumi, S. *J. Phys. Chem. A* **1998**, *102*, 3898–3906. (b) Wang, G.-W.; Murata, Y.; Komatsu, K.; Wan, T. S. M. *Chem. Commun.* **1996**, 2059–2060. (c) Komatsu, K.; Murata, Y.; Wang, G.-W.; Wan, T. S. M. In *Recent Advances in the Chemistry and Physics of Fullerenes and Related Materials*; Kadish, K. M., Ruoff, R. S., Eds.; The Electrochemical Society: Pennington, NJ, 1966; pp. 1200–1211. (d) Schick, G.; Kampe, K.-D.; Hirsch, A. *J. Chem. Soc., Chem. Commun.* **1995**, 2023–2024.

22. A linear relationship between E_{red}s and MO levels has also been reported for 1,2-cycloadducts: Suzuki, T.; Maruyama, Y.; Akasaka, T.; Ando, W.; Kobayashi, K.; Nagase, S. *J. Am. Chem. Soc.* **1994**, *116*, 1359–1363.
23. (a) Reetz, M. T.; Bingel, C.; Harms, K. *J. Chem. Soc., Chem. Commun.* **1993**, 1558–1560. (b) Maas, G.; Weber, H. M.; Exner, R.; Salbeck, J. *J. Phys. Org. Chem.* **1990**, *3*, 459–469. (c) Bruce, M. I.; Humphery, P. A.; Skelton, B. W.; White, A. H. *Aust. J. Chem.* **1986**, *39*, 165–169. (d) LeGoff, E.; LaCount, R. B. *Tetrahedron Lett.* **1964**, 1161–1164. (e) LeGoff, E.; LaCount, R. B. *J. Am. Chem. Soc.* **1963**, *85*, 1354–1355. (f) Boyd, R. H. *J. Am. Chem. Soc.* **1963**, *85*, 1555–1561. (g) Matsumura, S.; Seto, S. *Chem. Pharm. Bull. (Tokyo)* **1963**, *11*, 126–128.
24. Direct measurements of the electrical conductivity of $\mathbf{4}^+t\text{-BuC}_{60}^-$ in the absence of inorganic ions suffered from poor accuracy because of slow rate of dissolution of the hydrocarbon salt, which allowed deterioration of the sample before dissolution was complete.
25. The limiting molar ionic conductivity (λ_0) for K^+ is 14.69 S cm^2/mol in DMSO at 25°C: Gopal, R.; Shanker Jha, J. *J. Phys. Chem.* **1974**, *78*, 2405–2407. From this value and the Λ_0 of $t\text{-BuC}_{60}^-K^+$ (25.7 S cm^2/mol), the λ_0 for $t\text{-BuC}_{60}^-$ is calculated to be 11.0 S cm^2/mol.
26. The IR, Vis–NIR, and ^{1}H NMR spectra of $\mathbf{4}^+t\text{-BuC}_{60}^-$ have been reported in a preliminary communication (Ref. 19b).
27. Gutmann, V. *The Donor–Acceptor Approach to Molecular Interactions*; Plenum: New York, 1978 (Chapter 2).
28. (a) Arnett, E. M.; Amarnath, K.; Harvey, N. G.; Cheng, J.-P. *J. Am. Chem. Soc.* **1990**, *112*, 344–355. (b) Arnett, E. M.; Amarnath, K.; Harvey, N. G.; Cheng, J. P. *Science* **1990**, *247*, 423–430.
29. Arnett has shown that the sensitivities of the heat of C–C bond heterolysis in sulfolane toward the pK_{R^+} of the cationic component differ significantly depending on whether the carbocation is secondary or tertiary (Ref. 28). See also: Arnett, E. M.; Chawla, B.; Amarnath, K.; Whitesell Jr., L. G. *Energy Fuels* **1987**, *1*, 17–23.
30. (a) Akasaka, T.; Suzuki, T.; Maeda, Y.; Ara, M.; Wakahara, T.; Kobayashi, K.; Nagase, S.; Kako, M.; Nakadaira, Y.; Fujitsuka, M.; Ito, O. *J. Org. Chem.* **1999**, *64*, 566–569. (b) Kusukawa, T.; Ando, W. *J. Organomet. Chem.* **1998**, *561*, 109–120. (c) Kusukawa, T.; Ando, W. *J. Organomet. Chem.* **1998**, *559*, 11–22. (d) Kusukawa, T.; Ando, W. *Organometallics* **1997**, *16*, 4027–4029. (e) Kusukawa, T.; Ando, W. *Angew. Chem., Int. Ed. Engl.* **1996**, *35*, 1315–1317.
31. Although protonation at C-4 is kinetically favored, the 1,2-adduct is thermodynamically more stable than the 1,4-adduct. Thus, the protonation of $t\text{-BuC}_{60}^-$ often results in a mixture of both isomers (Refs. 6 and 8).
32. Stewart, J. J. P. *J. Comput. Chem.* **1989**, 209–263.
33. *Handbook of Chemistry and Physics*; Weast, R. C., Ed.; 67th ed.; CRC Press: Boca Raton, FL, 1987; p. E51.